



Neutron beam filter system for fast neutron cross-section measurement at the ANNRI beamline of MLF/J-PARC

2021 Nuclear Data Section Encouragement Award

G. Rovira^{1*}, O. Iwamoto¹, A. Kimura¹, S. Nakamura¹, N. Iwamoto¹, S. Endo¹, T. Katabuchi², K. Terada², Y. Kodama², H. Nakano², J. Hori³, Y. Shibahara³

1) Japan Atomic Energy Agency

2) Laboratory for Advanced Nuclear Energy, Tokyo Institute of Technology

3) Institute for Integrated Radiation and Nuclear Science, Kyoto University

Table of Contents

1. Accuracy Improvement of nuclear data for MAs.
2. MLF facility. Double-bunch mode of J-PARC
3. Neutron Filtering Technique
4. Neutron Filtering Experimental Setup
5. Experimental Results
6. Monte-Carlo Simulation
7. Standard Cross Section Results
8. Minor Actinides Cross Section Results
9. Conclusions

Accuracy improvement of nuclear data for MAs

Recent research trends are focused on the development of **Transmutation Facilities** for the treatment of **Nuclear Waste**. Convert the long-term component of Nuclear Waste (**Minor Actinides**) into **stable nuclei**.

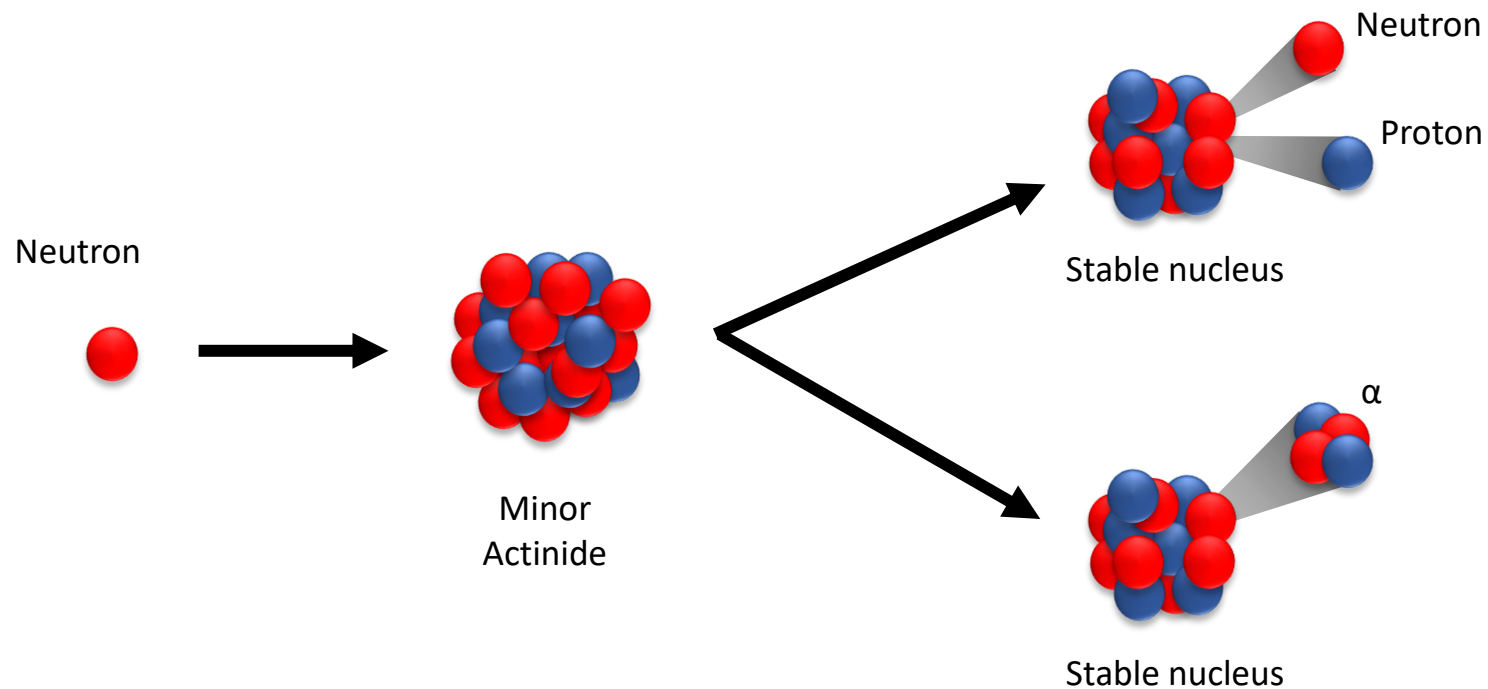


Fig. 1 Diagram of the nuclear transmutation process for minor actinides.

Accuracy improvement of nuclear data for MAs

Minor Actinides are usually **unstable radionuclides**, hence, it is **difficult** to measure nuclear reaction probabilities for such nuclei.

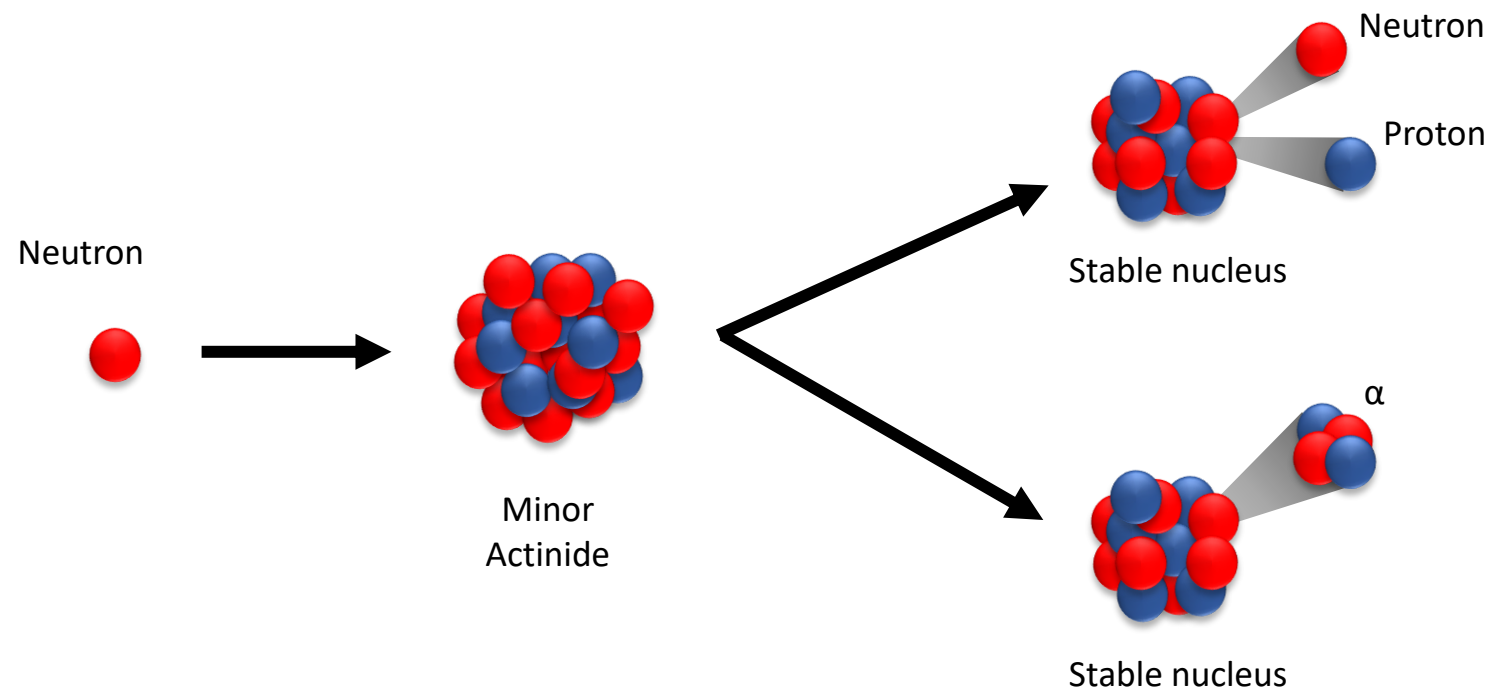


Fig. 1 Diagram of the nuclear transmutation process for minor actinides.

Accuracy improvement of nuclear data for MAs

Accelerator-Driven System (ADS) is a proposed sub-critical facility to perform the **nuclear transmutations of MAs**

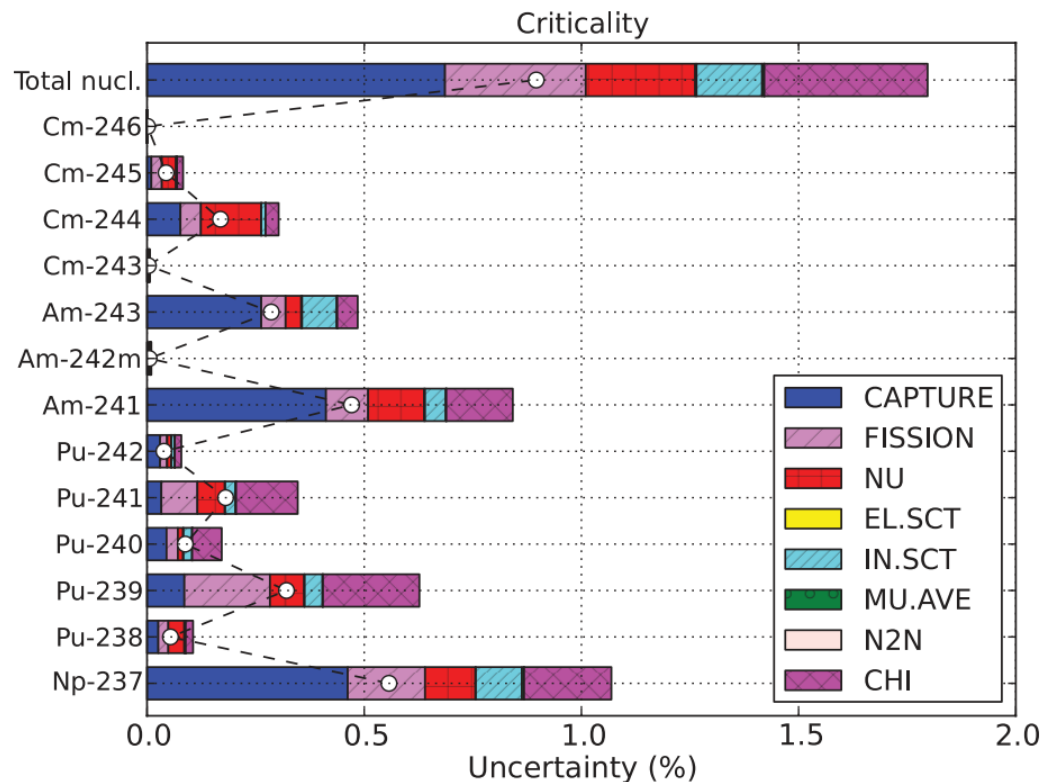


Fig. 2 Uncertainties by reaction and nuclide of ADS criticality*

*H.Iwamoto et al. J. Nucl. Sci. Technol., 2013; 50(8):856-862.

- Although achieved through **fission**, **other reaction channels** also need to be considered
- **Accurate data** for the **neutron capture cross section** of **MAs** is important for the **ADS** design
- **Improvement** required for **keV-neutron data**

Accuracy improvement of nuclear data for MAs

An accuracy improvement of the current **nuclear data** for the **neutron capture cross section of MAs** in the **keV-region** is needed.



More accurate experiments for
Minor Actinides are required

Accura

Experiments with **keV-neutrons** at **ANNRI** are currently **impractical** due to the **double-bunch**

MAAs

An accur

structure of the neutron beam

neutron

capture cross section of MAAs in the keV-region is needed.

The **double-bunch** problem in the ANNRI beamline has to be **resolved** in order to perform further accurate neutron capture experiments with **keV-neutrons**

More accurate  experiments for

“Study on accuracy improvement of fast-neutron capture reaction data of long-lived MAAs for development of nuclear transmutation systems” project

Project Overview

Joint collaboration project by **JAEA**, **Tokyo Tech** and **Kyoto Univ.**

Focused on improving the accuracy of **nuclear data** for minor actinides in the **keV** region for ^{237}Np , ^{241}Am and ^{243}Am

Divided in 4 parts:

- Neutron Beam Filter Develop.

- JAEA

- Sample Characteristic Assay

- Kyoto Univ.

- Neutron Capture Measurement

- Tokyo Tech
- ^{237}Np , ^{241}Am and ^{243}Am

- Theoretical Reaction Model Study

- JAEA

MLF Facility

In the MLF facility, **pulsed neutrons** are generated by **pulsed protons** shot to a **Hg target** via **spallation reactions**. In previous years, the **J-PARC** accelerator was operated in **single bunch mode**.

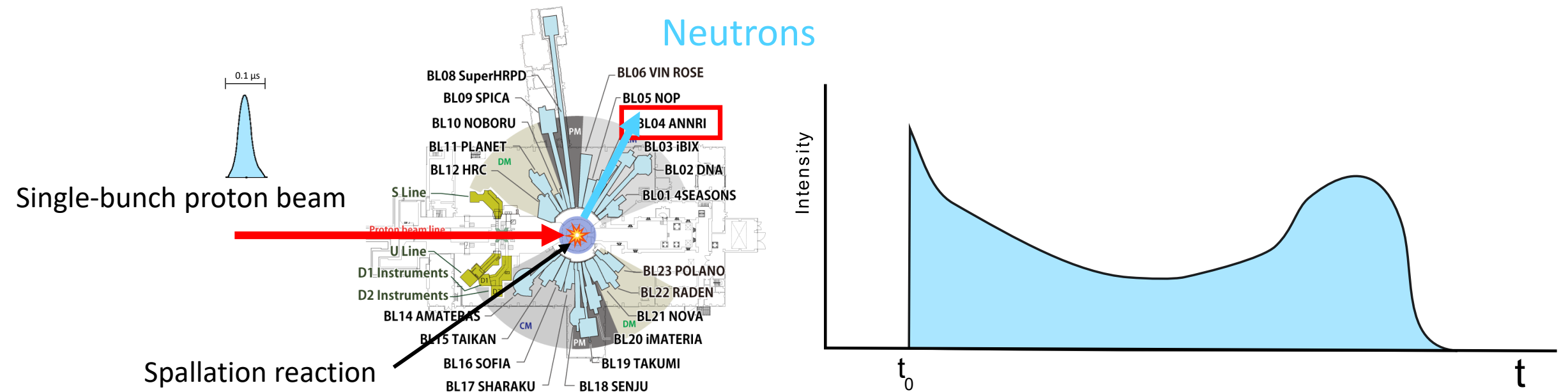


Fig. 3 Schematic of the MLF facility and the single-bunch neutron generation process.

*<https://mlfinfo.jp/ja/blmap.html>

Double-bunch mode of J-PARC

Recently, the **J-PARC** accelerator was switched onto **double-bunch mode** where two proton bunches are shot with a time difference of **0.6 μ s** to generate neutrons every 40 ms (25 Hz).

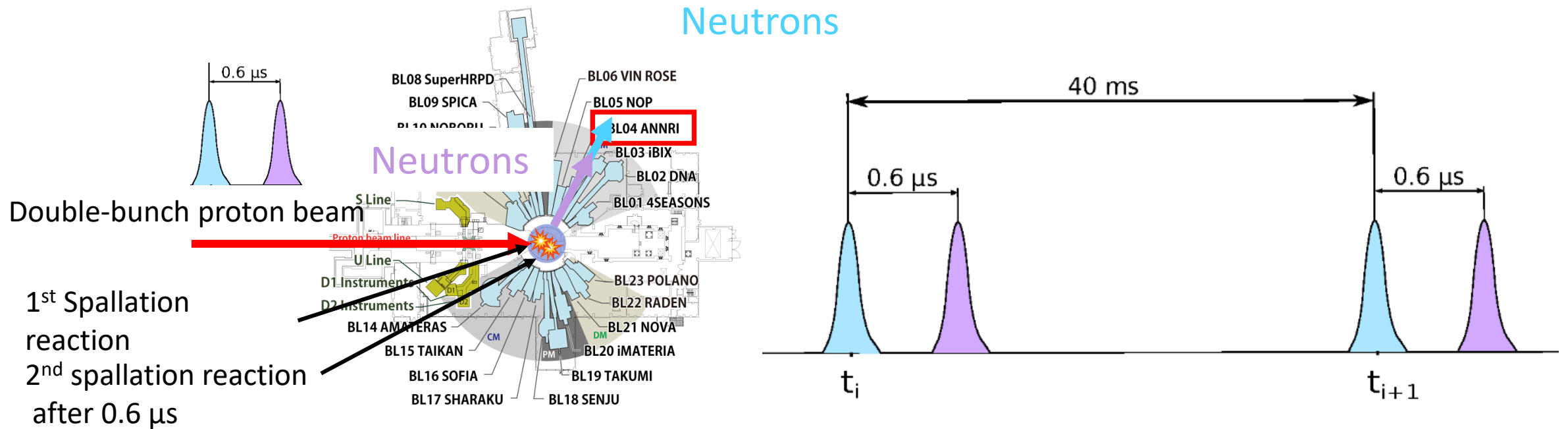


Fig. 4 Schematic of the MLF facility and the double-bunch neutron generation process.

*<https://mlfinfo.jp/ja/blmap.html>

Double-bunch mode of J-PARC

In time-of-flight (TOF) experiments, the energy of the neutrons is determined from **timing measurements**.

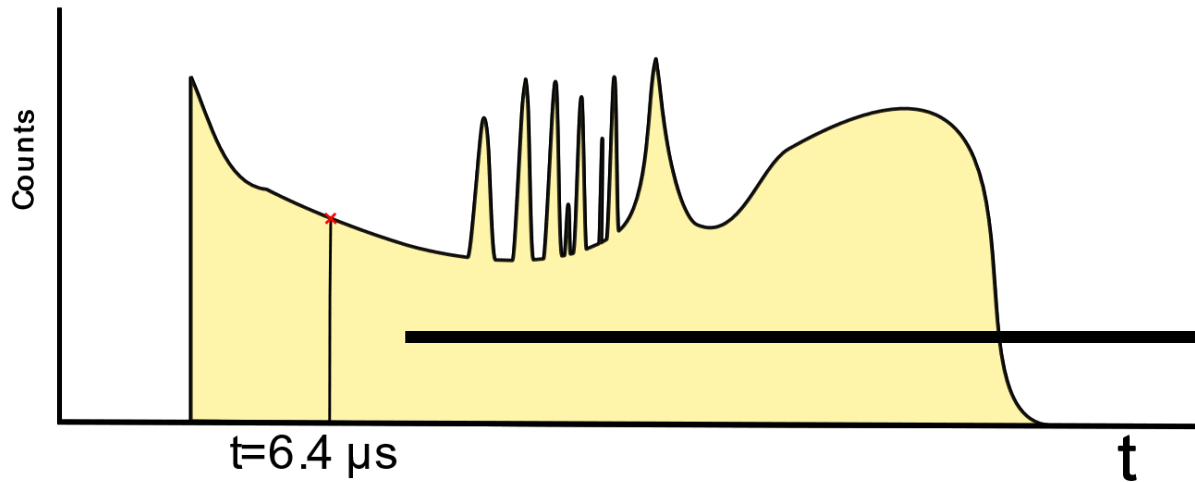


Fig. 5 Example of raw events detected in a capture experiment at ANNRI with the NaI(Tl) spectrometer in single-bunch mode

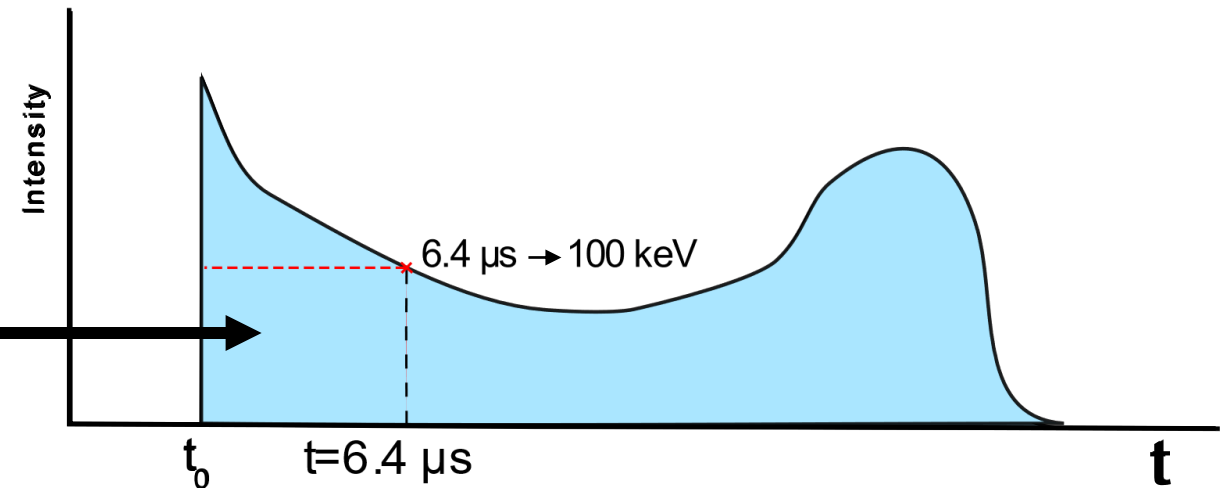


Fig. 6 Schematic of the neutron flux generated in the single-bunch mode

Double-bunch mode of J-PARC

In time-of-flight (TOF) experiments, the energy of the neutrons is determined from **timing neutrons in d** **It is impossible to determine the originating proton pulse of the detected neutron events for keV neutrons** **ities for keV-**

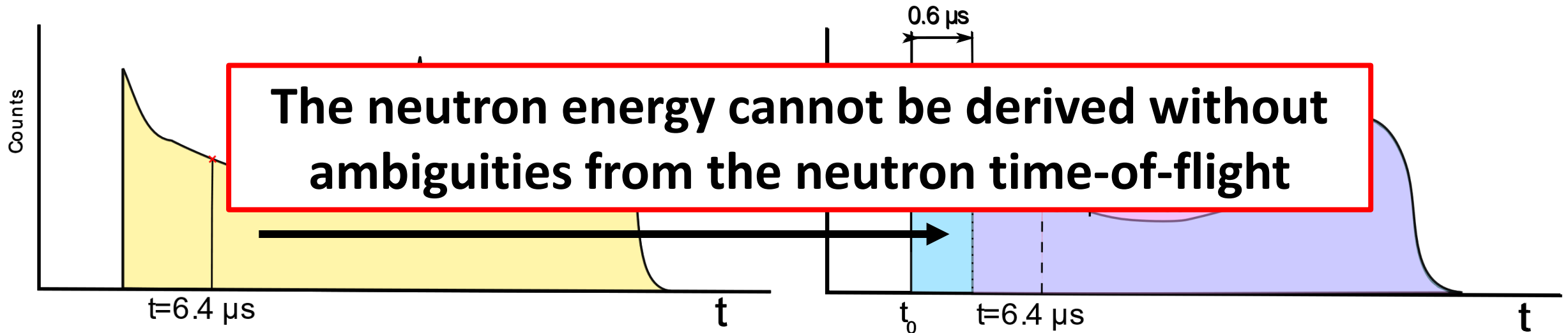
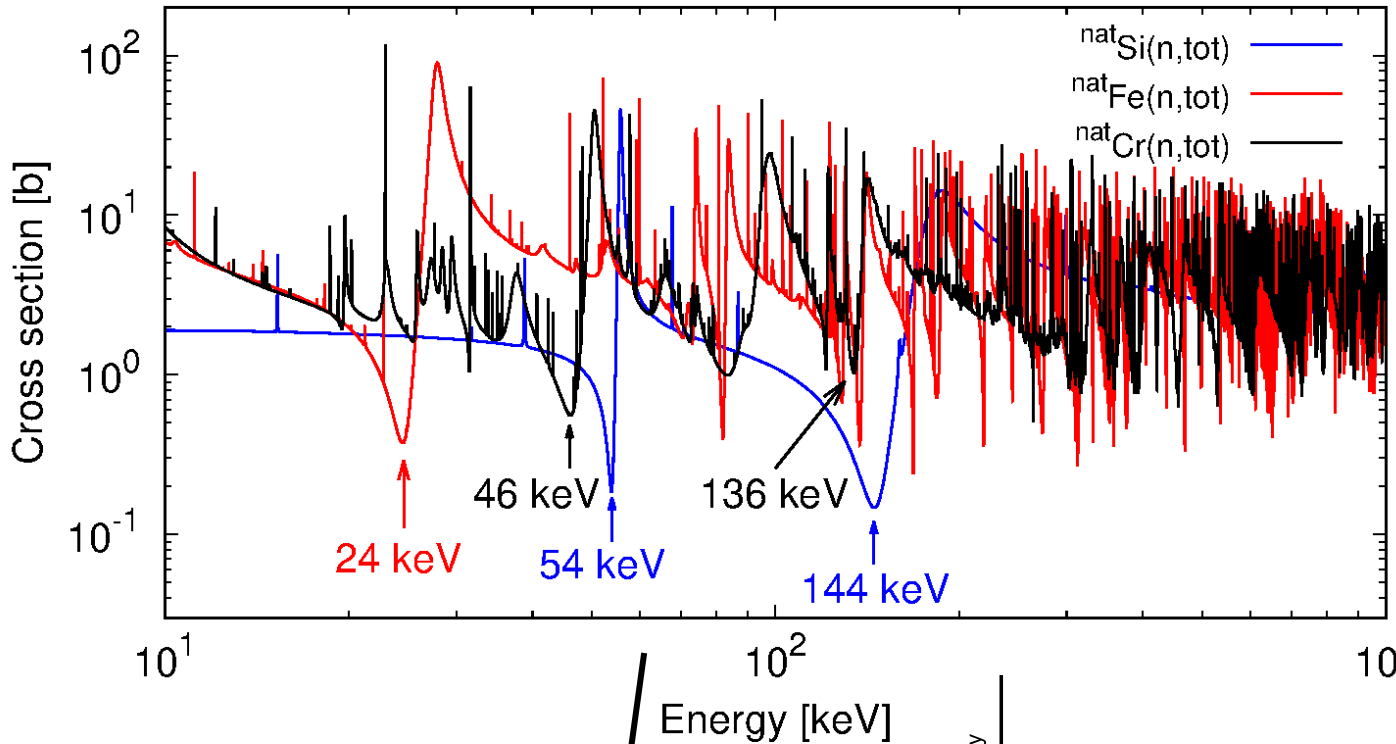


Fig. 7 Example of raw events detected in a capture experiment at ANNRI with the NaI(Tl) spectrometer in double-bunch mode

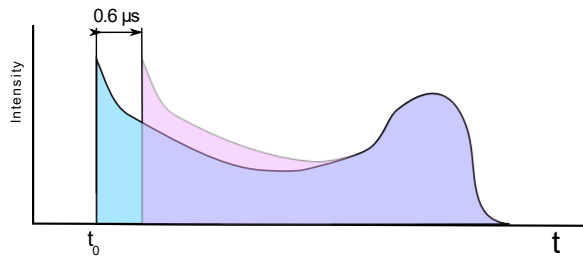
Fig. 8 Schematic of the neutron flux generated in the double-bunch mode. For example, events detected with time-of-flight ($t=6.4 \mu\text{s}$) can have two different neutron energies of 100 or 120 keV depending on the originating proton pulse.

Neutron

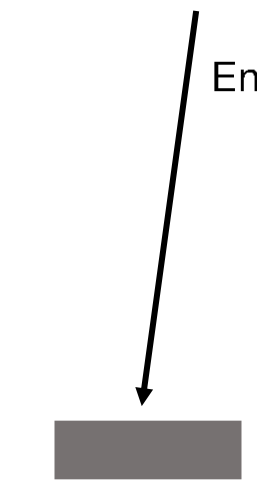
The **Neutron** double-bunch reactors. Quasi-monoenergetic neutron beams that present a



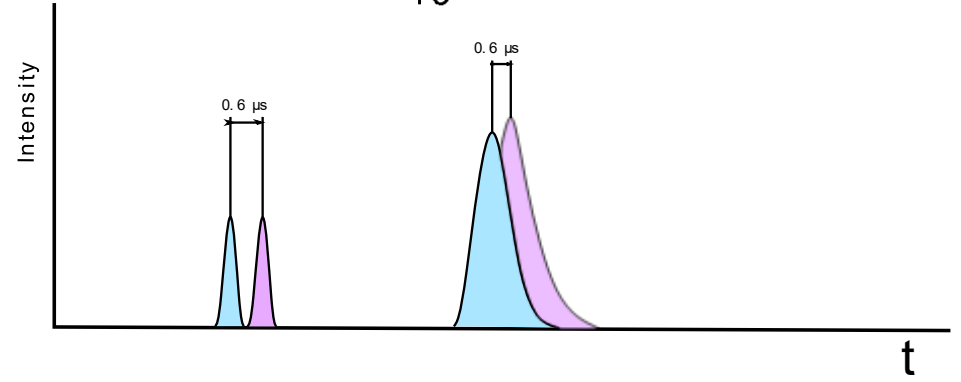
The effects of the applied to nuclear and using materials filtration.



Incident neutron flux



Filter material



Filtered neutron beam

Filtered neutron beam

Fig. 9 Neutrons with the energy of the **sharp minimum** of the filter material can **pass through** to create **quasi-monoenergetic neutron peaks**

Neutron Filtering System Setup

Filter materials (Fe, Si and Cr) were introduced in the rotary collimator of the ANNRI beamline. Configurations of 20 cm of Fe and Si; 15 cm of Cr were tested.

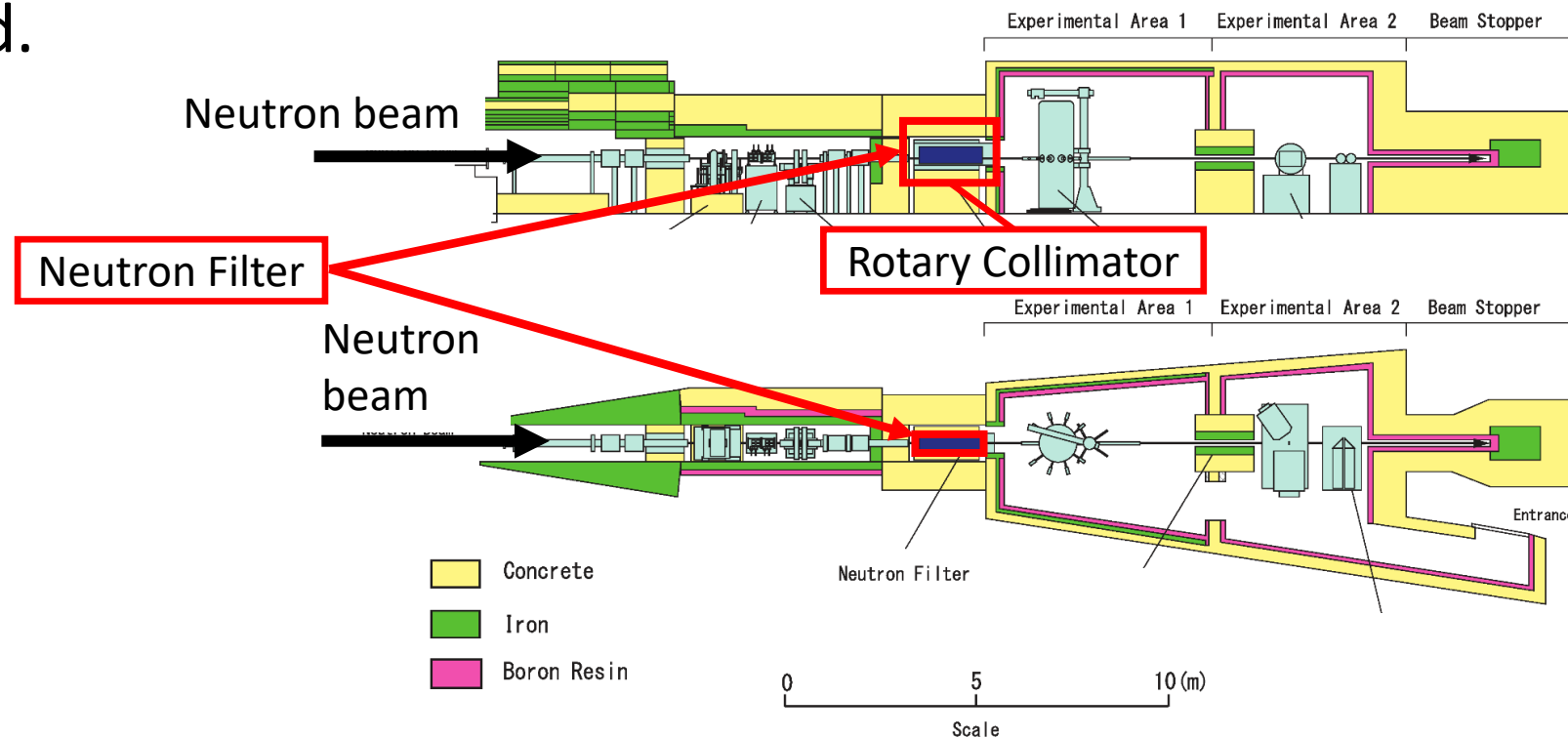


Fig. 10 Overview of the ANNRI beamline. The **filter material** was inserted into the **rotary collimator**.

Experimental Setup

The time distribution of the filtered neutron flux was obtained by using both **Li-glass detectors** and a **NaI(Tl) spectrometer**. **Standard Au neutron capture cross-section** measurement to assess the **filter performance**.

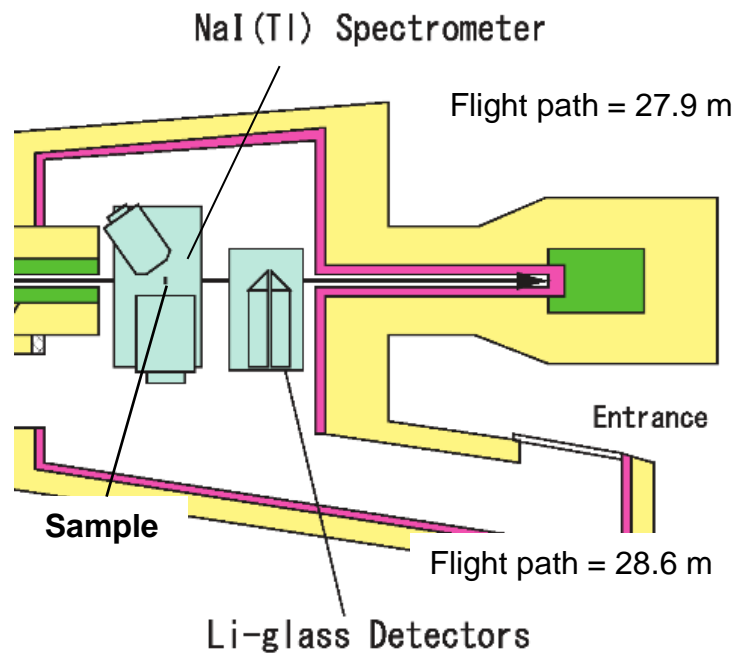


Fig. 11 Overview of the **NaI(Tl) spectrometer** and **Li-glass detectors** in the ANNRI beamline.

FILTERED NEUTRON FLUX DETERMINATION

NaI(Tl) spectrometer

- **Boron sample**
- $^{10}\text{B}(n,\alpha)^7\text{Li}$ reaction

Li-glass detectors

- Direct neutron flux measurement

PERFORMANCE ASSESSMENT IN CAPTURE EXPERIMENTS

NaI(Tl) spectrometer

- **Au sample**
- Neutron capture **γ -ray** measurement
- **Au neutron capture cross-section** used as **standard cross-section** for verification. It has been **measured extensively** in the past and its evaluated (JENDL-4.0) results are deemed **highly reliable**.

Experimental Results

The **neutron flux** derived from experiments with **Li-glass detectors** and a **NaI(Tl) spectrometer** present **very good agreement**. The difference in time is due to the different detector position.

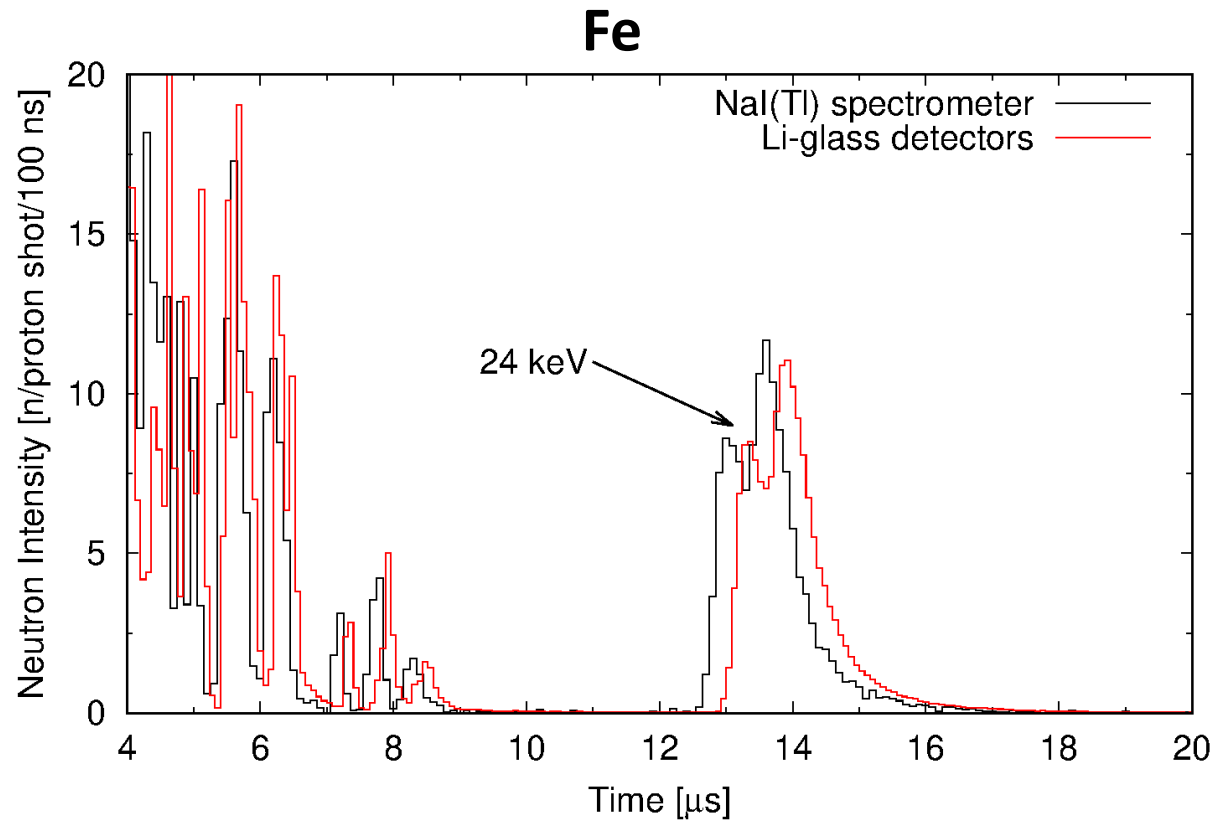


Fig. 12 Filtered neutron beam through **20 cm of Fe** measured by **Li-glass detectors** and a **NaI(Tl) spectrometer**

Experimental Results

The **neutron flux** derived from experiments with **Li-glass detectors** and a **NaI(Tl) spectrometer** present **very good agreement**. The difference in time is due to the different detector position.

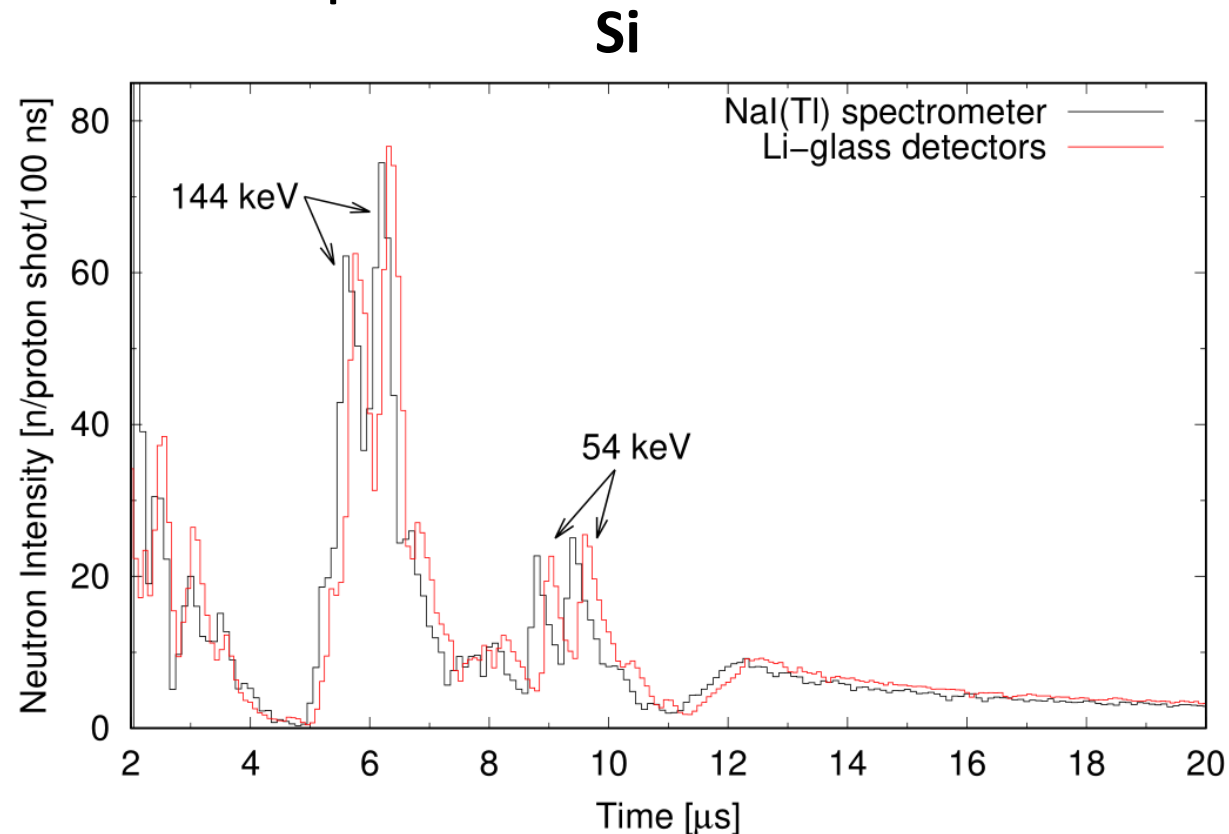
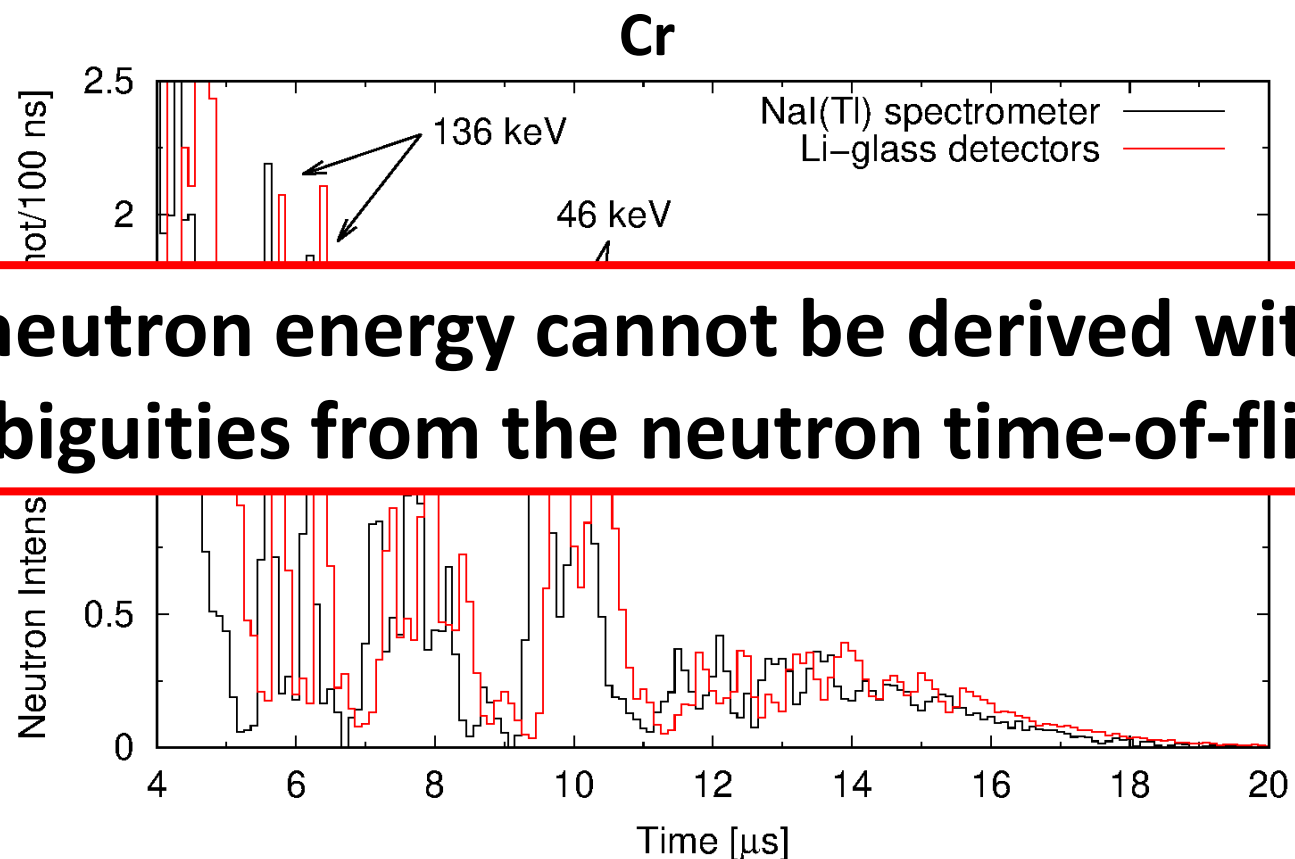


Fig. 13 Filtered neutron beam through **20 cm of Si** measured by **Li-glass detectors** and a **NaI(Tl) spectrometer**

Experimental Results

The peaks at the energies of **24, 46, 54, 136** and **144 keV** are clearly **isolated**.
Time to energy conversion is presents **ambiguities**.



The neutron energy cannot be derived without ambiguities from the neutron time-of-flight

Fig. 14 Filtered neutron beam through **15 cm of Cr** measured by **Li-glass detectors** and a **NaI(Tl) spectrometer**

Monte-Carlo Simulation

The **neutron energy distribution** within the filtered peaks can be derived through Monte-Carlo simulations with **PHITS**, unfolded with the **resolution function** of the ANNRI beamline

Experimental results were **simulated** for the filter materials (**Fe, Si and Cr**)

In PHITS, **simultaneous** calculations of neutron time and energy are performed

The simulation **precision** was evaluated by comparing the **simulated** neutron time distribution to the **experimental** neutron time distribution for each filter

Monte-Carlo Simulation

Two-dimensional results for the neutron **time** and **energy** distributions were obtained with **PHITS**. Simulation results were assessed by comparing the **simulated** neutron time distribution with the **experimental** results.

Fe

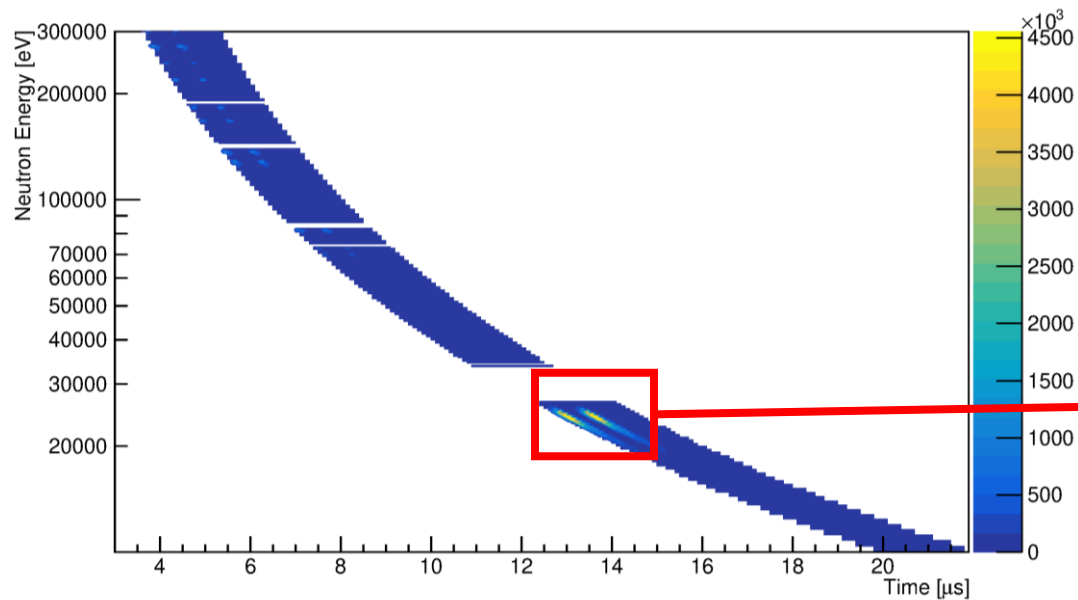


Fig. 15 Two-dimensional simulation results with **20 cm of Fe**

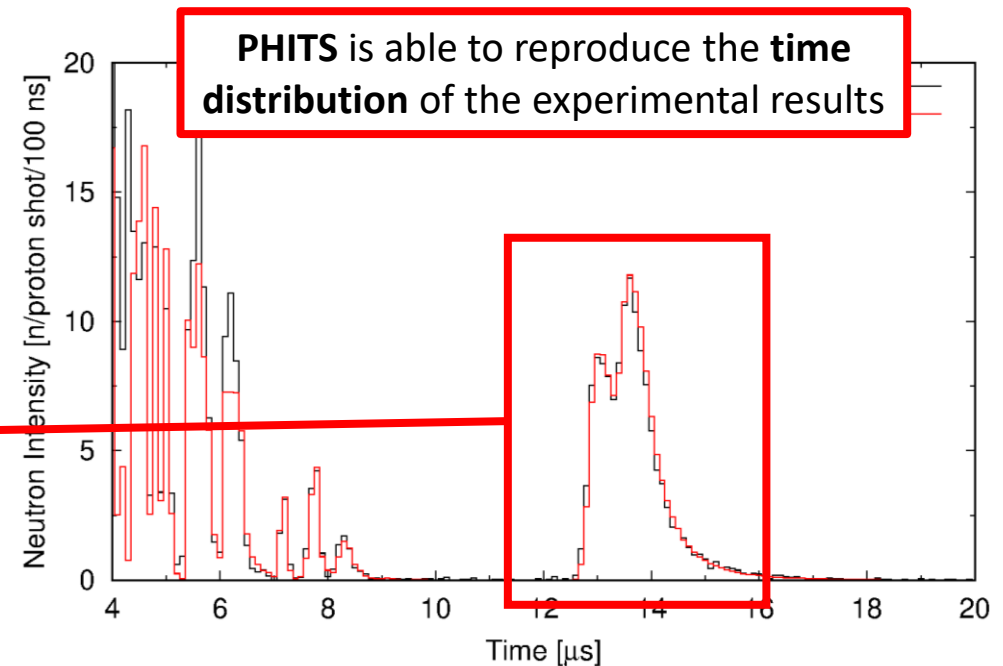


Fig. 16 Time distribution simulation results with **20 cm of Fe** compared to experimental results.

Monte-Carlo Simulation

Two-dimensional results for the neutron **time** and **energy** distributions were obtained with **PHITS**. Simulation results were assessed by comparing the **simulated** neutron time distribution with the **experimental** results.

Si

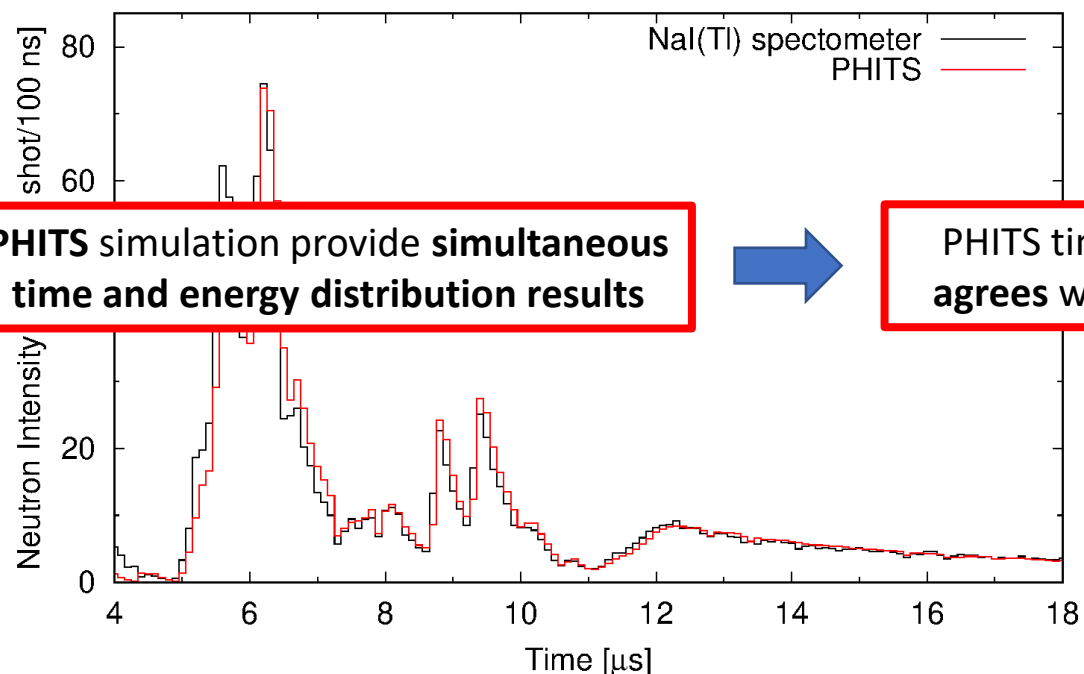


Fig. 17 Time distribution simulation results with **20 cm of Si** compared to experimental results.

Cr

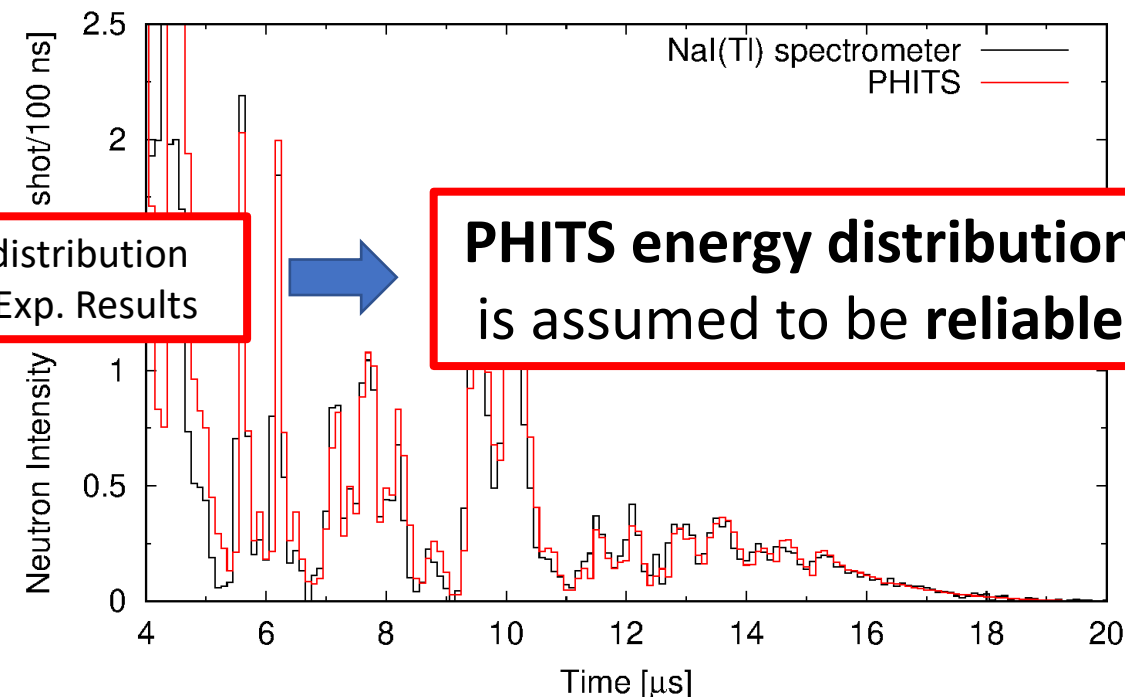


Fig. 18 Time distribution simulation results with **15 cm of Cr** compared to experimental results.

Monte-Carlo Simulation – Energy distribution

Only **events** from the **gated areas** were analyzed to obtain the **neutron energy distribution** at the peak position without the influence neutrons filtered at other energies.

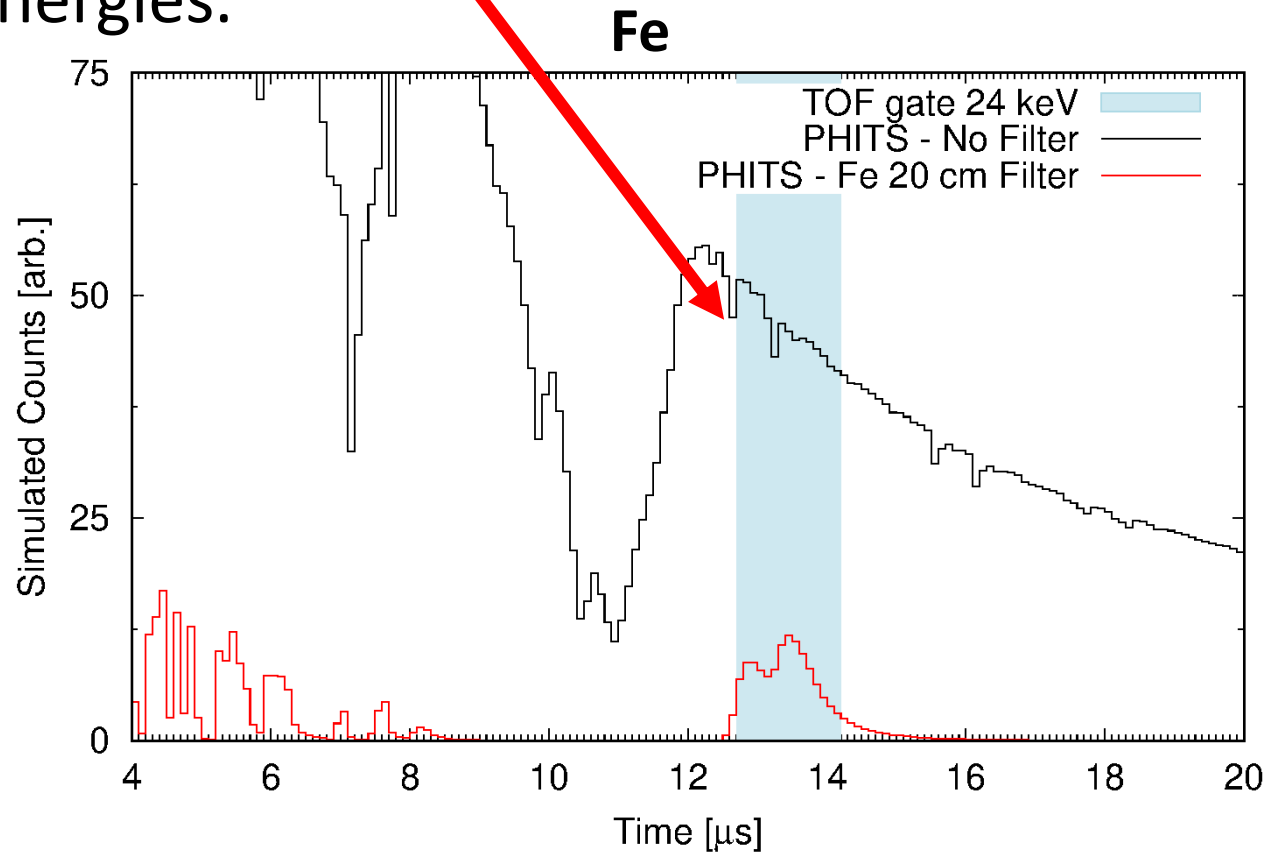


Fig. 19 TOF gate to wrap the **24 keV** filtered neutron peak with the **Fe** filter

Monte-Carlo Simulation – Energy distribution

Only **events** from the **gated areas** were analyzed to obtain the **neutron energy distribution** at the **peak position** without the influence neutrons filtered at other energies.

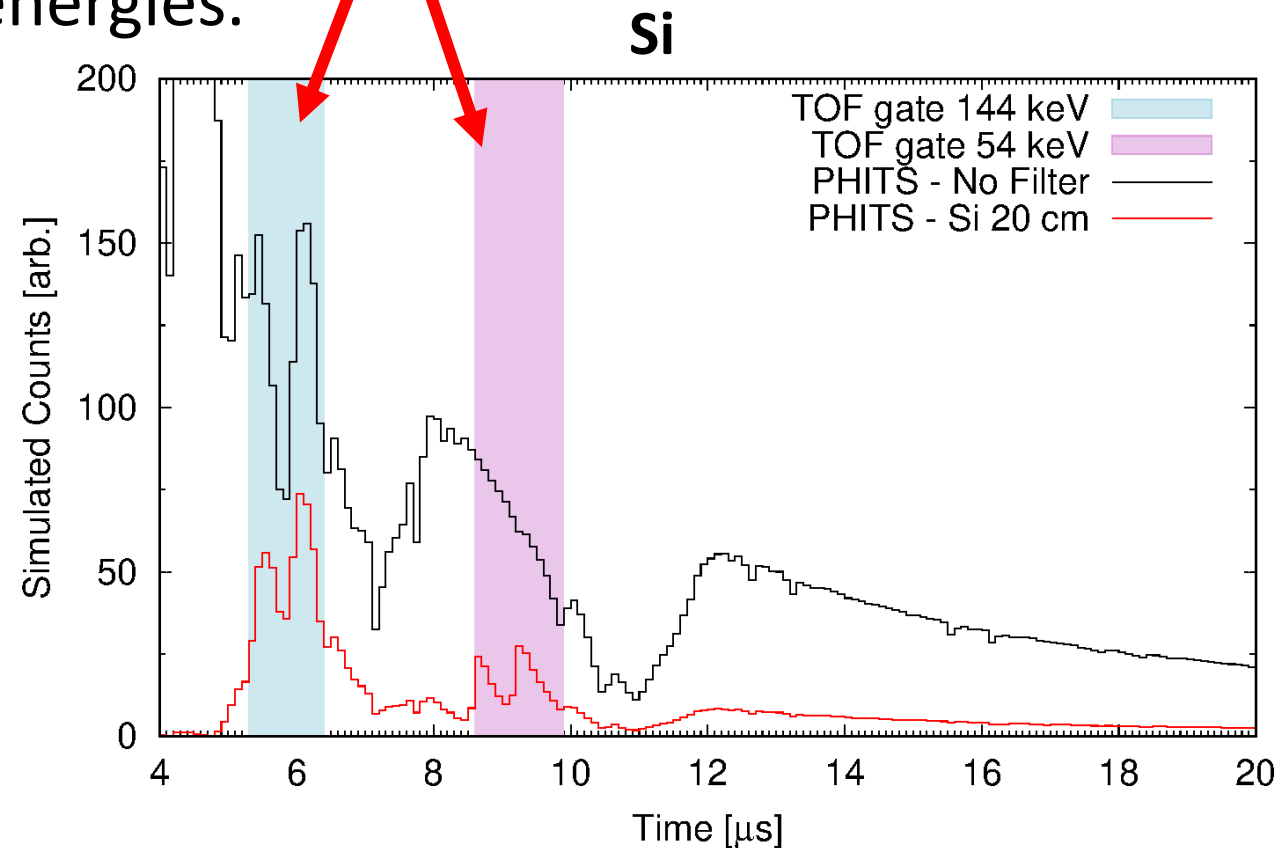


Fig. 20 TOF gates to wrap the **54 and 144 keV** filtered neutron peaks with the **Si filter**

Monte-Carlo Simulation – Energy distribution

Only **events** from the **gated areas** were analyzed to obtain the **neutron energy distribution** at the peak position without the influence neutrons filtered at other energies.

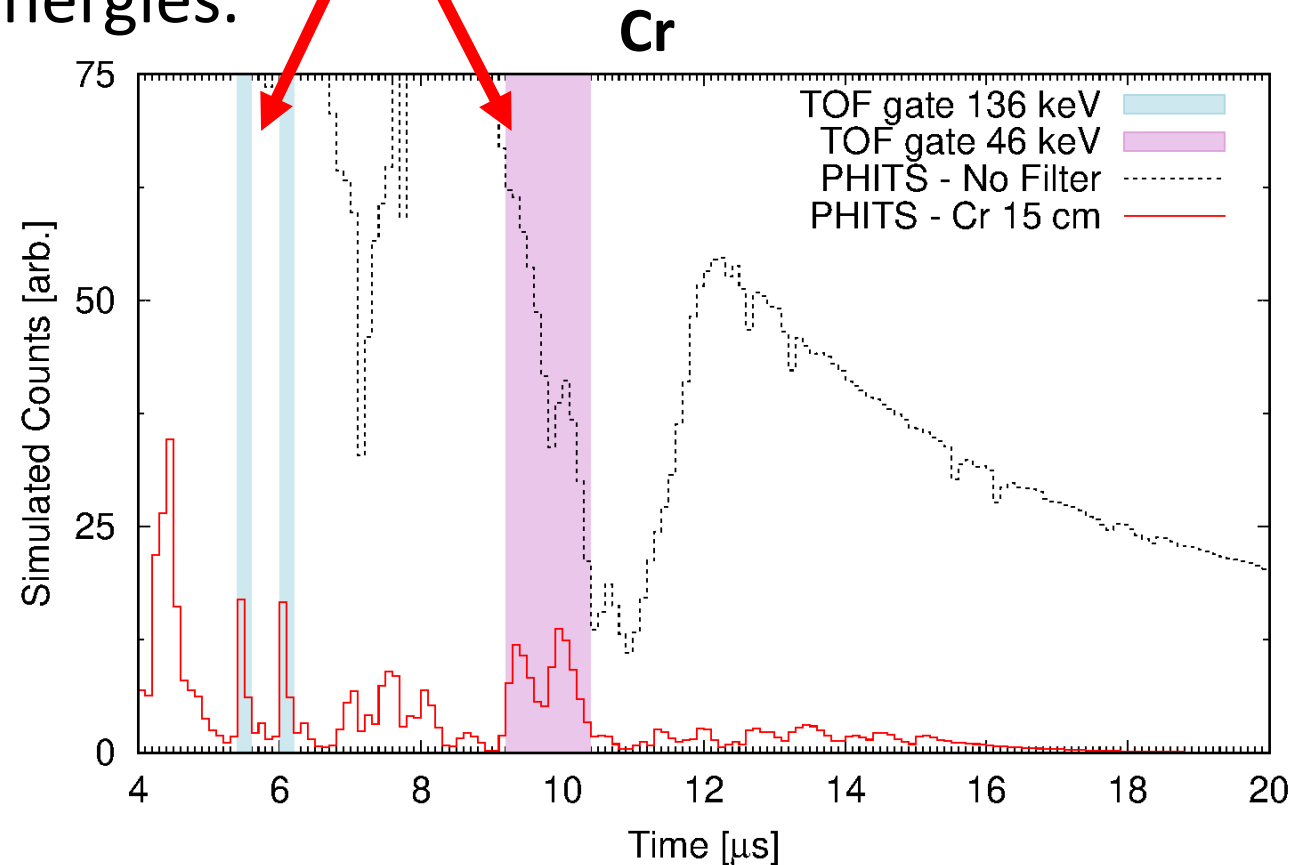


Fig. 21 TOF gates to wrap the **46 and 136 keV** filtered neutron peaks with the **Cr filter**

Monte-Carlo Simulation – Energy distribution

The **neutron energy distribution** was obtained by gating the PHITS results at each filtered peak.

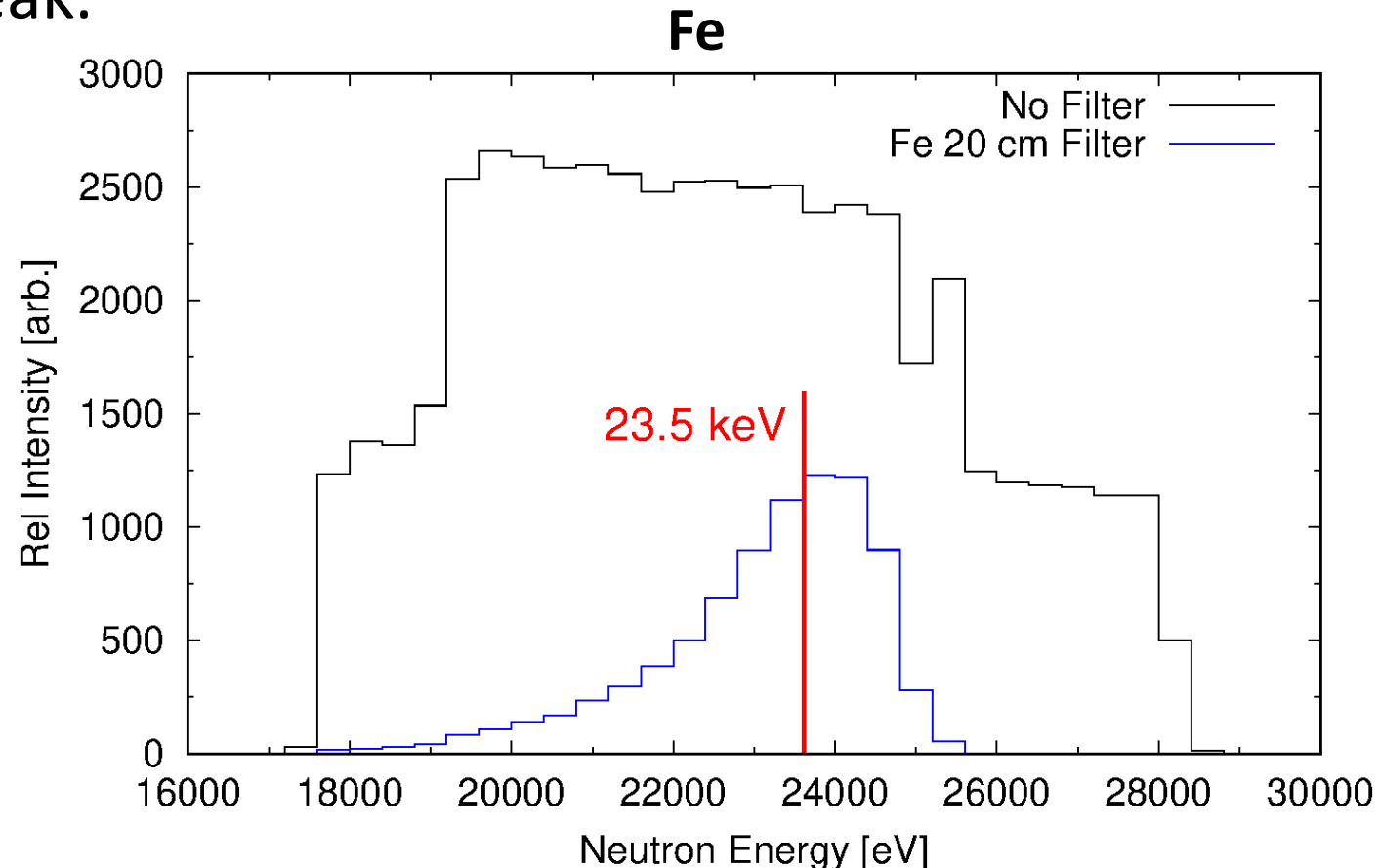


Fig. 22 **Energy distribution** of the **filtered neutron beam (blue)** and its **energy centroid (red)** compared to the **energy distribution without filter (black)**

Monte-Carlo Simulation – Energy distribution

The **neutron energy distribution** was obtained by gating the PHITS results at each filtered peak

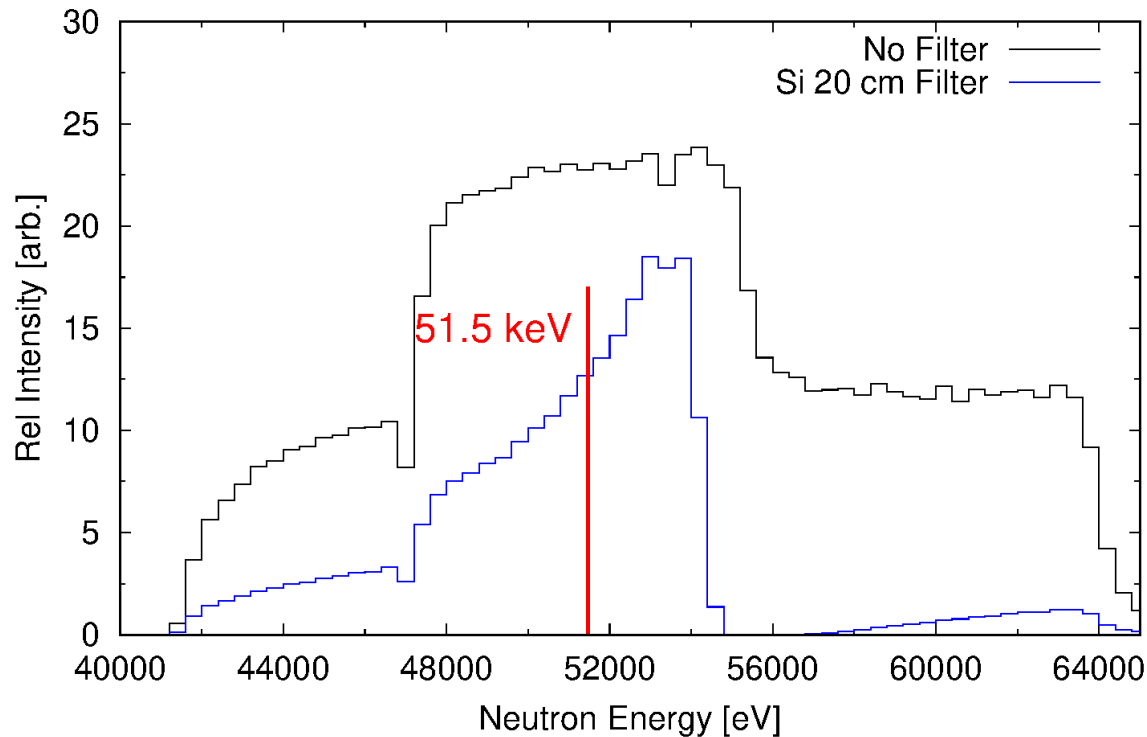


Fig. 23 Energy distribution of the 54 keV filtered neutron beam (blue) and its energy centroid (red) compared to the energy distribution without filter (black)

Si

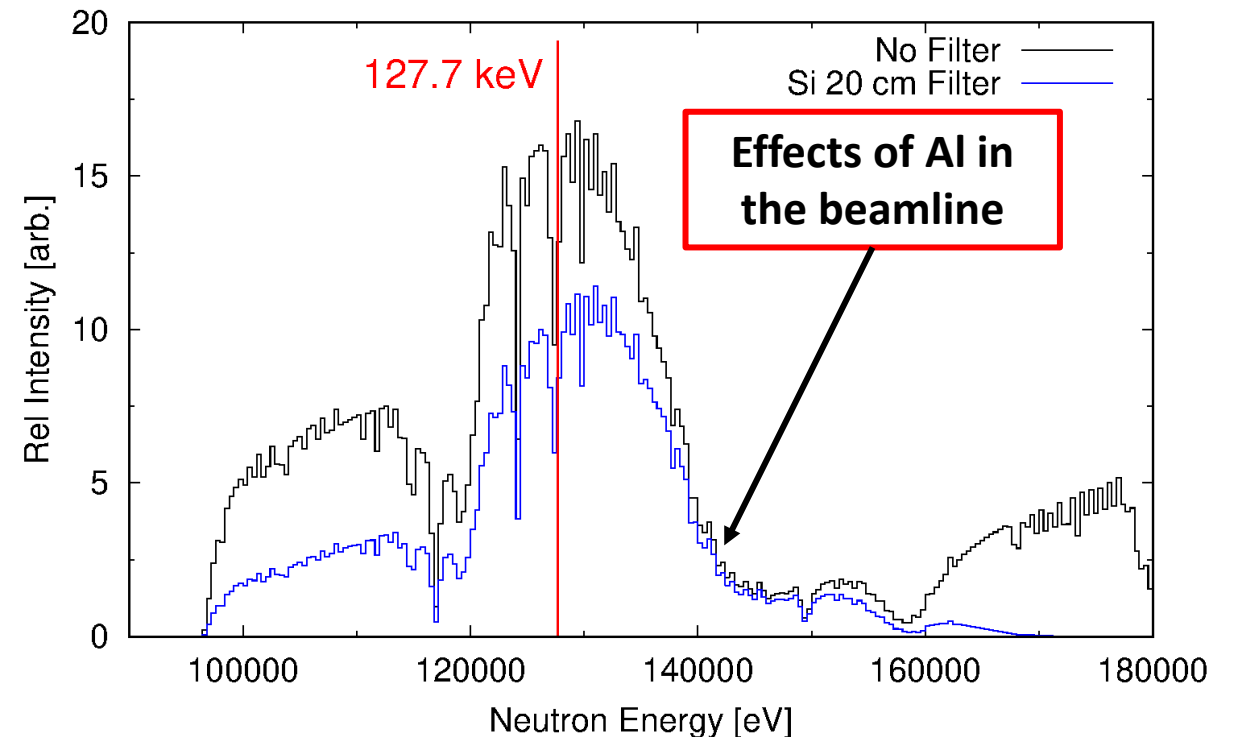


Fig. 24 Energy distribution of the 144 keV filtered neutron beam (blue) and its energy centroid (red) compared to the energy distribution without filter (black)

Monte-Carlo Simulation – Energy distribution

The **neutron energy distribution** was obtained by gating the PHITS results at each filtered peak

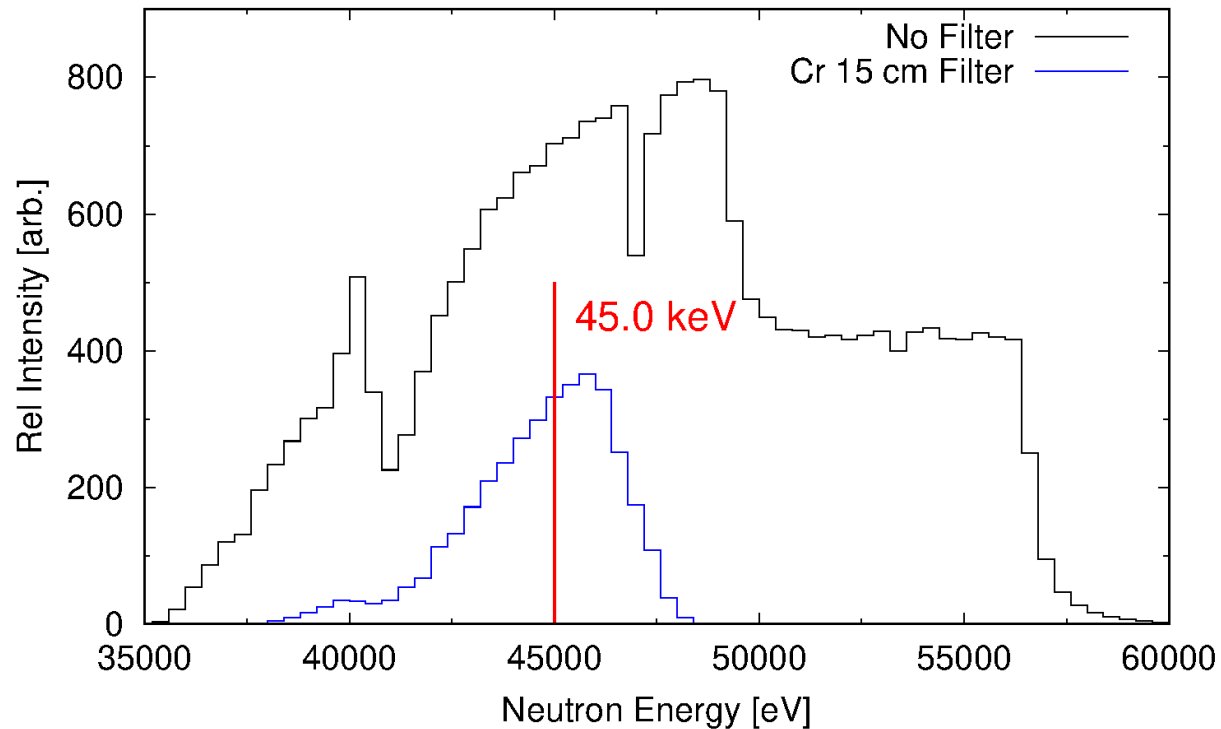


Fig. 25 Energy distribution of the **46 keV filtered neutron beam (blue)** and its energy centroid (**red**) compared to the energy distribution without filter (**black**)

Cr

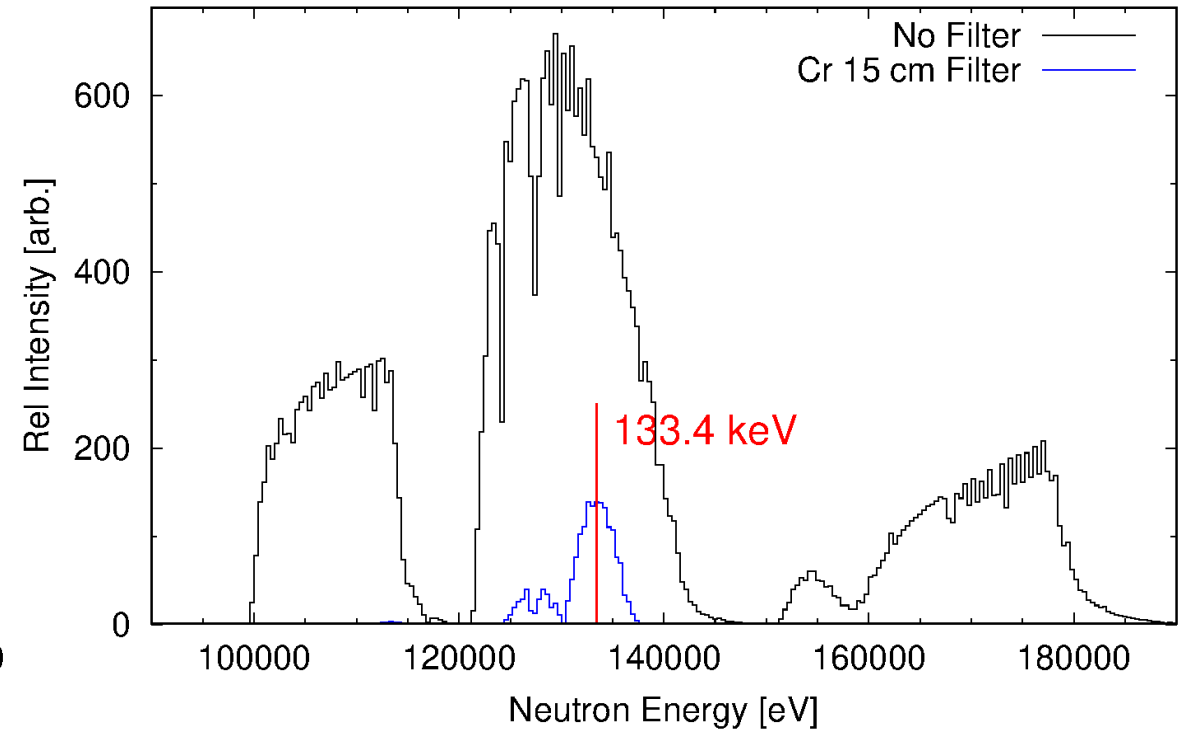


Fig. 26 Energy distribution of the **136 keV filtered neutron beam (blue)** and its energy centroid (**red**) compared to the energy distribution without filter (**black**)

Standard Cross Section Results

The $^{197}\text{Au}(n,\gamma)$ cross-section was determined using the **Fe**, **Si** and **Cr** filtered peaks. Results contain **total uncertainties below 5%**.

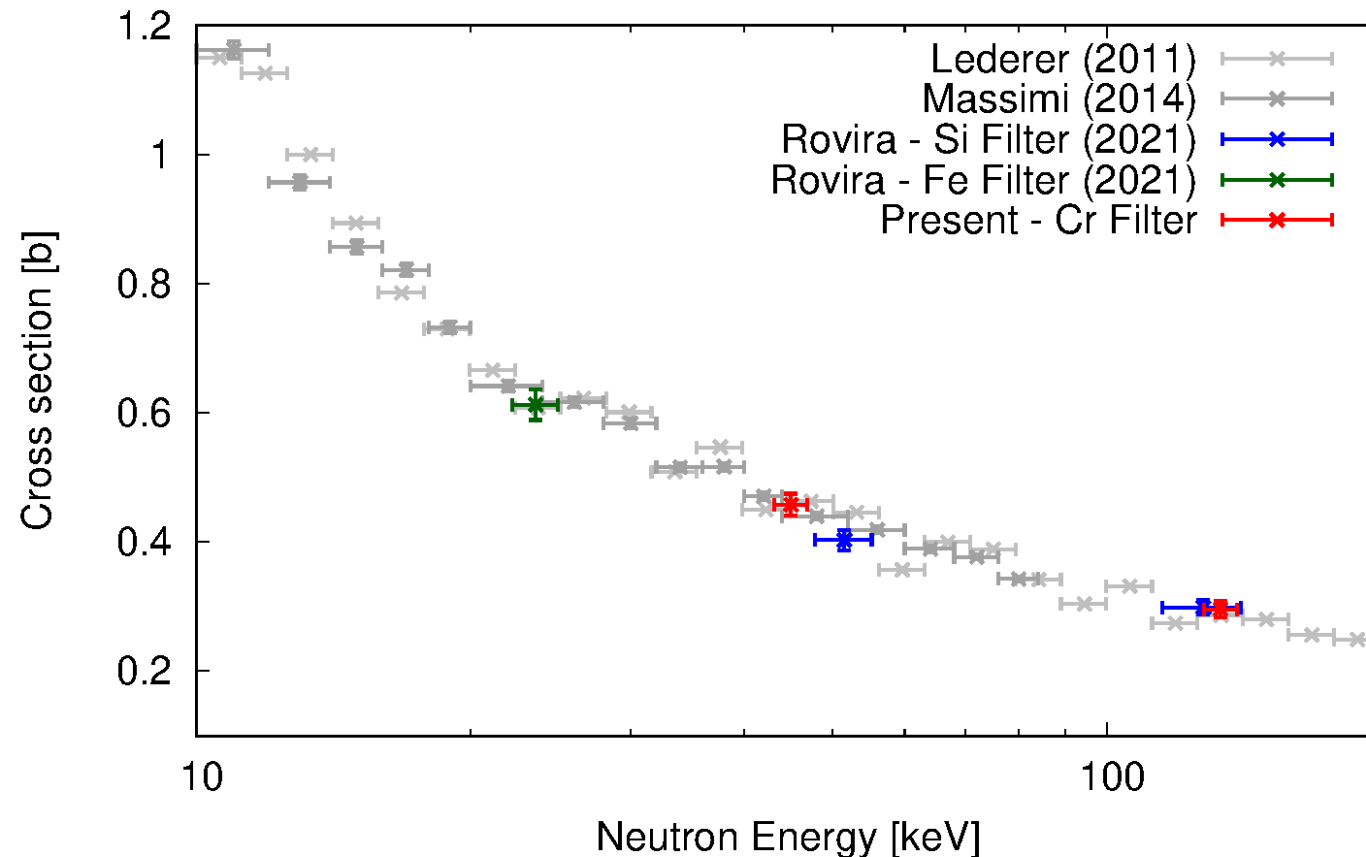
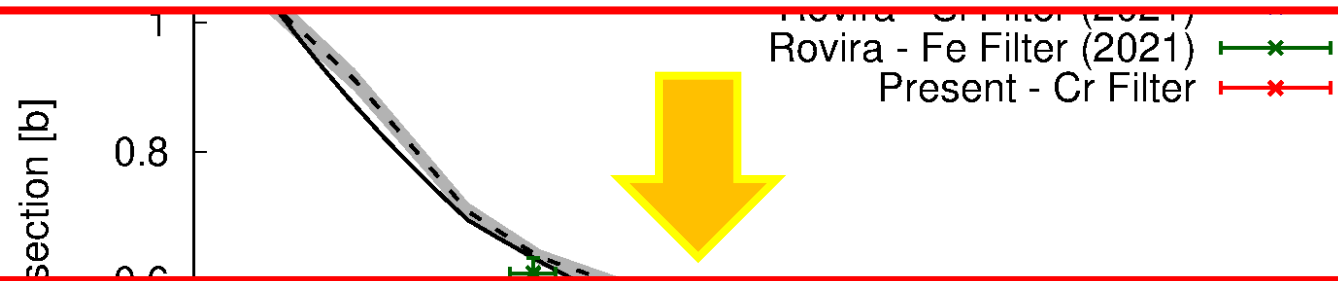


Fig. 27 Cross section results for ^{197}Au using the **Fe filter (green)**, **Si filter (blue)** and **Cr filter (red)** compared with the latest **TOF experimental results**.

Standard Cross Section Results

The peak
The **present** cross section results with the **Fe, Si and Cr** filters **agree** within uncertainties with both **experimental** and **evaluated** nuclear data



The **Neutron Filtering System** is a **viable solution** in order to bypass the double-bunch structure and measure neutron induced cross-sections for **keV-neutrons**.

Fig. 28 Cross section results for ^{197}Au using the **Fe filter (green)**, **Si filter (blue)** and **Cr filter (red)** compared with the evaluated data from **JENDI-4.0** and the **IAEA Standard** libraries.

Minor Actinides Cross Section Results

The **first** cross section results have already been published in the work of **Kodama* et al.** The neutron capture cross section of ^{243}Am was measured at the energy of **23.5 keV** with the **Fe** filter.

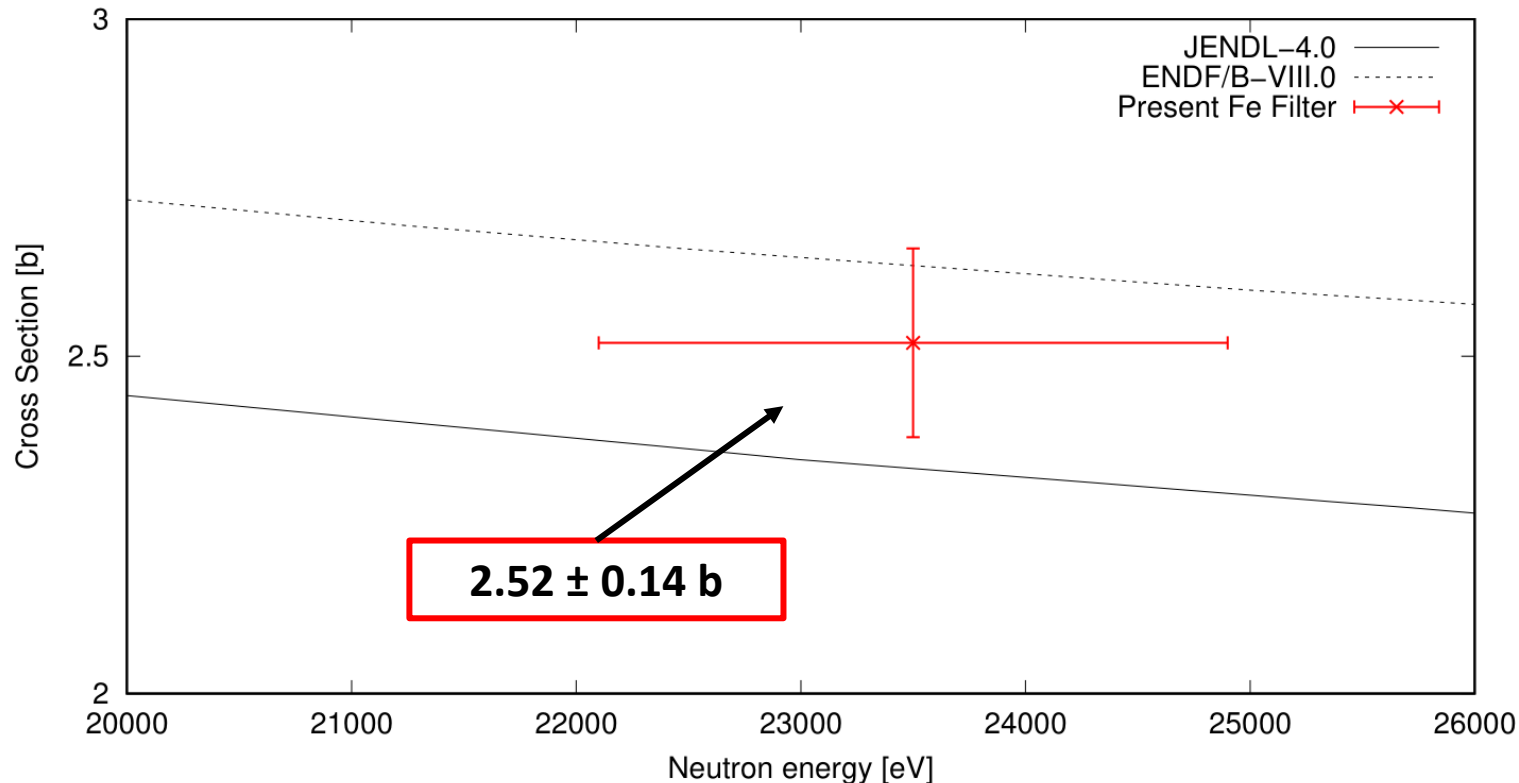


Fig. 29 Cross section results for ^{243}Am at **23.5 keV** with the **Fe** filter from the work of **Kodama* et al.** compared with evaluated results from **JENDL-4.0** and **ENDF/B-VIII.0**

*Kodama et al. J. Nucl. Sci and Technol. Rapid Communication, 2021.

Minor Actinides Cross Section Results

Preliminary neutron capture cross section of ^{241}Am measured at the energy of **23.5 keV** with the **Fe** filter.

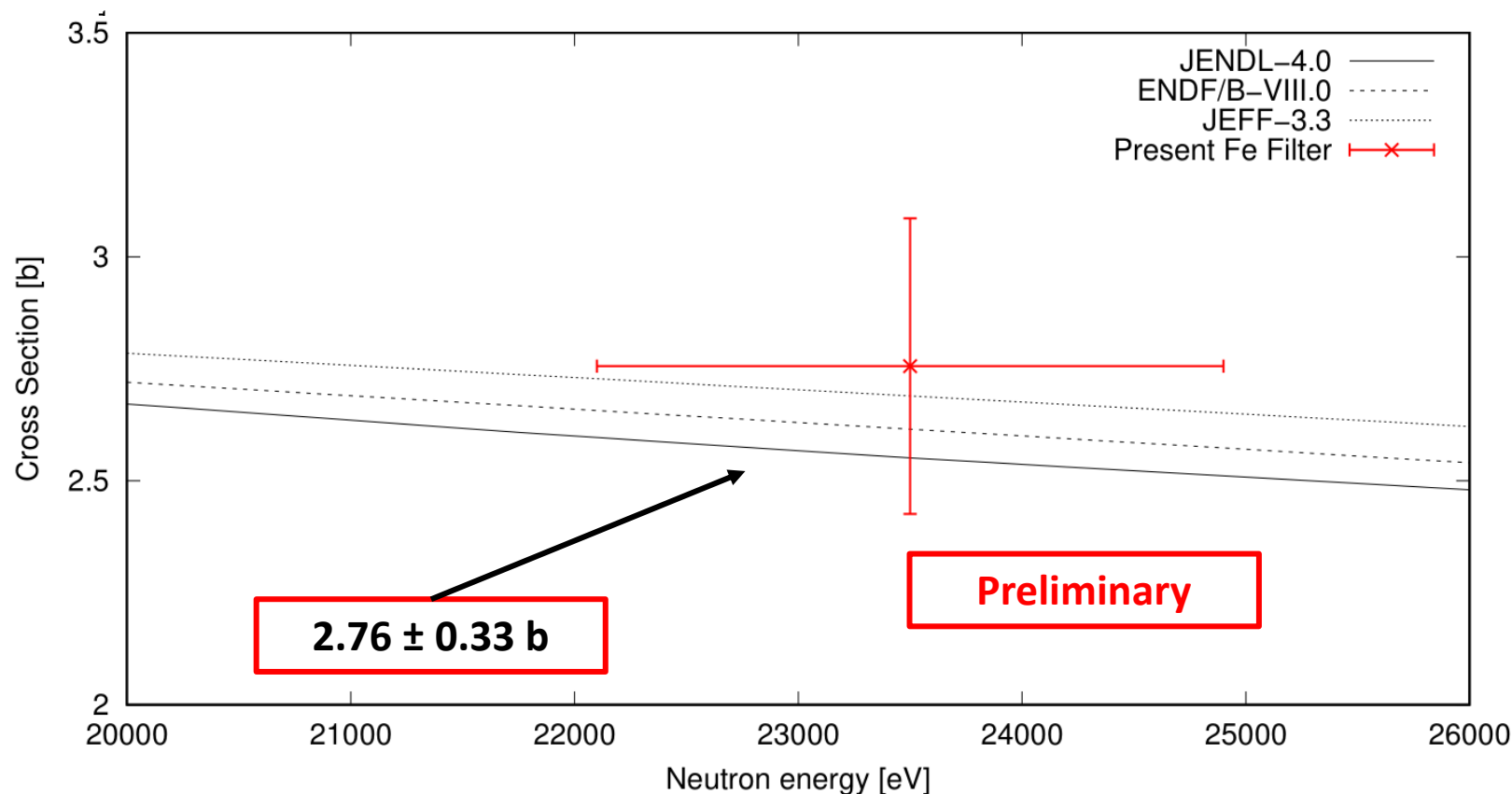


Fig. 30 Preliminary cross section results for ^{241}Am at **23.5 keV** with the **Fe** filter compared with evaluated data libraries

Conclusions

- **Developed a Neutron Filtering System to bypass the effects of the double-bunch mode**
 - Filtering system is able to **tailor quasi-monoenergetic neutron peaks** with Fe, Si and Cr with **peaks of 23.5, 45.0, 51.5, 127.7 and 133.4 keV**
 - The **time distribution** of the filtered neutron flux was accurately determined by experiments with both **Li-glass detectors** and a **NaI(Tl) spectrometer**
 - **Monte-Carlo simulations** are able to **reproduce** the experimental results
 - **Neutron energy distributions** of the filtered peaks determined from simulations
 - **Performance in neutron-induced cross-section** measurements **verified** by the good agreement with **experimental** and **evaluated** data for ^{197}Au .
- **Cross-section measurements with fast neutrons can be performed using the Neutron Filtering System at ANNRI**
 - First cross section results for minor actinides (^{243}Am) already published

ACKNOWLEDGMENT

This work is supported by MEXT. The neutron experiments at the MLF of the J-PARC were performed under the user program (Proposal No. 2018A0213, 2018B0195 and 2020P0100)

This work was awarded the 2021 Encouragement Award by the Nuclear Data Subcommittee of the Atomic Energy Society of Japan